Journal for ImmunoTherapy of Cancer

Targeting of colorectal cancer organoids with zoledronic acid conjugated to the anti-EGFR antibody cetuximab

Roberto Benelli,[1] Delfina Costa,[1] Laura Salvini,[2] Samuele Tardito,[1] Francesca Tosetti,[1] Federico Villa,[1] Maria Raffaella Zocchi,[3] Alessandro Poggi [1]

To cite: Benelli R, Costa D, Salvini L, *et al*. Targeting of colorectal cancer organoids with zoledronic acid conjugated to the anti-EGFR antibody cetuximab. *Journal for ImmunoTherapy of Cancer* 2022;**10**:e005660. doi:10.1136/jitc-2022-005660

► Additional supplemental material is published online only. To view, please visit the journal online (http://dx.doi.org/10.1136/jitc-2022-005660).

Accepted 17 October 2022

[1]Molecular Oncology and Angiogenesis Unit, IRCCS Ospedale Policlinico San Martino, Genova, Italy
[2]Technologies Facilities, Fondazione Toscana Life Sciences, Siena, Italy
[3]Division of Immunology, Transplants and Infectious Diseases, IRCCS San Raffaele Scientific Institute, Milan, Italy

Correspondence to
Dr Alessandro Poggi; alessandro.poggi@hsanmartino.it

ABSTRACT

Background Antibody-drug conjugates (ADC) are essential therapeutic options to treat solid and hematological cancers. The anti-epidermal growth factor-receptor (EGFR) antibody cetuximab (Cet) is used for the therapy of colorectal carcinoma (CRC). Anti-CRC Vδ2 cytolytic T lymphocytes can be elicited by the priming of tumor cells with the aminobisphosphonate zoledronic acid (ZA) and consequent presentation of isopentenyl pyrophosphates through butyrophilin (BTN) family members such as BTN3A1 and BTN2A1. A major drawback that impairs the targeting of ZA to CRC is the bone tropism of aminobisphosphonates.

Methods The phosphoric group of ZA was linked to free amino groups of Cet in the presence of imidazole following the labeling of phosphoric groups of DNA to amino groups of proteins. The generation of Cet-ZA ADC was confirmed by matrix assisted laser desorption ionization mass spectrometry and inductively coupled plasma-mass spectrometry analysis. Thirteen CRC organoids were obtained with a chemically defined serum-free medium in Geltrex domes. Proliferation and activation of cytolytic activity against CRC organoids by Vδ2 T cells was detected with flow cytometry, crystal violet and cytotoxic probe assays and image analysis. Immunohistochemistry and quantification of BTN3A1 or BTN2A1 expression and the number of tumor infiltrating Vδ2 T cells in CRC were performed by automatic immunostaining, whole slide scanning and computerized analysis of digital pathology imaging.

Results The novel ADC Cet-ZA was generated with a drug antibody ratio of 4.3 and displayed a reactivity similar to the unconjugated antibody. More importantly, patient-derived CRC organoids, or CRC tumor cell suspensions, could trigger the expansion of Vδ2 T cells from peripheral blood and tumor infiltrating lymphocytes when primed with Cet-ZA. Furthermore, Cet-ZA triggered Vδ2 T cell-mediated killing of CRC organoids. The expression of BTN3A1 and BTN2A1 was detected not only in CRC organoids but also in CRC specimens, together with a considerable amount of tumor infiltrating Vδ2 T cells.

Conclusions These findings are proof of concept that the Cet-ZA ADC can be used to target specifically CRC organoids and may suggest a new experimental approach to deliver aminobisphosphonates to EGFR$^+$ solid tumors.

WHAT IS ALREADY KNOWN ON THIS TOPIC

⇒ Antibody-drug conjugates (ADC) approved for cancer treatment allow the direct targeting of tumor cells by a therapeutic monoclonal antibody (mAb) with an anticancer drug. However, less than 1% of the currently administered ADC is expected to target the tumor.

WHAT THIS STUDY ADDS

⇒ We propose a new type of ADC, connecting zoledronic acid (ZA) with the anti-epidermal growth factor-receptor mAb cetuximab (Cet); ZA is known to activate antitumor Vδ2 T lymphocytes, but its employment in cancer therapy is limited by the bone tropism of the drug.

⇒ The most powerful characteristic of Cet-ZA ADC is the ability to select and expand Vδ2 T cells, driving them to colorectal cancer (CRC) organoids where they exert effective tumor cell killing though T-cell receptor activation and antibody dependent cytotoxic activity.

HOW THIS STUDY MIGHT AFFECT RESEARCH, PRACTICE OR POLICY

⇒ This as an additional tool in this field, resulting in a precise and effective targeting of CRC, favoring the development of a double-edged antitumor immune response that would amplify the therapeutic effect.

⇒ These findings give the proof of concept that the ZA-based ADC can be used to target specifically cancer cells and may suggest a new experimental approach to deliver aminobisphosphonates to the tumor site.

INTRODUCTION

The involvement of immune system in the control of solid tumors, including colorectal cancer (CRC), is aknowledged.[1–3] In particular, analysis of CRC with overall survival outcomes revealed intratumoral γδ T cells as a highly significant favorable prognostic immune population.[4–6] The involvement of these cells in CRC is also linked to a subset of these T lymphocytes residing within the

mucosa-associated lymphoid tissue in the gut.[7 8] The γδT lymphocytes can be activated on recognition of unprocessed non-peptide small molecules, including phosphoantigens derived from the mevalonate pathway in tumor cells.[7–9] Another remarkable activation signal is delivered via FcγRIIIa/CD16 that binds the IgG Fc triggering antibody-dependent cellular cytotoxicity (ADCC) against opsonized tumor cells.[7–9]

Synthetic pyrophosphate-containing compounds, including aminobisphosphonates (N-BPs), improve γδT-cell activation, with a consequent increased number of γδT cells in the blood, displaying antitumor activity.[9–11] Indeed, N-BPs, such as zoledronic acid (ZA), are chemically stable analogs of inorganic pyrophosphate that inhibit the farnesyl pyrophosphate synthase of the mevalonate pathway and upregulate isopentenyl pyrophosphate (IPP) accumulation, promoting the preferential growth of antitumor Vγ9Vδ2T cells in vitro and in vivo. For this immunostimulating property, besides the direct anticancer effects, different N-BPs have been tested in clinical trials.[9–11]

The ability to recognize IPP by Vγ9Vδ2T cells has been related to butyrophilin 3A1 (BTN3A1), characterized by the intracellular signaling domain B30.2, that binds IPP and drives the activation of Vγ9Vδ2T cells through conformational changes of the extracellular domains.[11–13] Recent evidence for the involvement of BTN2A1 as another important co-stimulating molecule included in IPP presentation to Vγ9Vδ2T cells, has been reported.[14] We have recently published that CRC cells (epithelial or mesenchymal) from tumor specimens, exposed to ZA, stimulate the expansion of Vδ2T cells with antitumor activity[15 16]; BTN3A1 is detected in most CRC at the tumor site, on epithelial and stromal cells, often close to areas infiltrated by Vδ2T lymphocytes.[15] Thus, N-BPs like ZA can conceivably be proposed in therapeutic schemes of CRC, provided a good expression of BTN3A1 on cells of the tumor microenvironment.

An important type of drugs stimulating the immune response, exploited also in anticancer therapy, is represented by monoclonal antibodies (mAb) able to elicit ADCC by immune cells bearing the FcγRI/II/III.[7–10] Different humanized mAb, such as the anti-epithelial growth factor receptor (EGFR) cetuximab (Cet), are used in Kras/Nras wild type CRC.[17 18] These therapeutic mAb would accomplish the double purpose of targeting cancer cells at the tumor site and amplify the immune response by the recruitment of different antitumor effector cell populations.[19 20] However, in second-line treatments, no survival advantage has been shown using either the chimeric Cet or the human panitumumab, and results in first-line treatments were reached only in combination with oxaliplatin.[17] In the last years, antibody-drug conjugates (ADC) have been synthesized and approved for cancer treatment: this strategy allows the direct targeting of tumor cells by a therapeutic mAb with an anticancer drug.[19–22] However, a few ADC have been approved by the US Food and Drug Administration and by the European Medicines Agency, probably due to a relatively low clinical success rate, while, at present, more than 50 other ADC are in clinical studies.[20] We propose a new type of ADC, connecting ZA (immunostimulating/anticancer properties) with Cet that recognizes a tumor target molecule and, in addition, can activate ADCC.

In this paper we show that: (1) Cet-ZA ADC is feasible and the covalent binding is reached exploiting the synthesis of phosporamidate (2) ZA conjugation does not alter Cet reactivity with EGFR and the Cet-ZA ADC maintains the same specificity of the native unconjugated antibody; (3) Cet-ZA ADC reacts with CRC-derived organoids, inducing IPP production; (4) Cet-ZA ADC can trigger Vδ2 T cells to grow and exert effective cytotoxic activity against CRC organoids; (5) in CRC, Vδ2 T lymphocytes can be found not only close to the tumor, but also inside the tumor where BTNs, in particular BTN3A1, are expressed.

METHODS

Production of Cet-ZA ADC

ZA (MW 272.09) was purchased from Selleckchem (Houston, Texas, USA) and Cet (Erbitux) was obtained as leftover of the therapeutic preparation used for patients suffering from CRC (kind gift from the Pharmacy Unit of IRCCS Ospedale Policlinico San Martino, Genoa). Cet-ZA ADC was prepared by Nanovex Biotechnologies (Asturias, Spain) as follows. Erbitux has been dialyzed to eliminate the excipients. The solutions of ZA and 1-ethyl -3-(3-dimethylaminopropyl) carbodiimide hydrochloride (EDC, Sigma-Aldrich, Missouri, USA) were prepared in 0.1M imidazole at pH 6±0.2 (with HCl 1N). ZA has been incorporated in the protein structure through the phosphoric groups of ZA according to the reactions reported to conjugate peptides and the free phosphoric acid of DNA.[23–26] Briefly, the following reactions can be defined (online supplemental figure 1): (1) ZA and EDC in a 100-fold molar excess (eg, 1 mg/mL of ZA and 100 mg/mL EDC) at room temperature (RT) generating an acylurea intermediate; (2) this acylurea reacts with imidazole generating a phosphorimidazolide; (3) this phosphorimidazolide reacts with free amino groups of aminoacids of the Erbitux added to the solution in a 585-fold molar excess (eg, 1 mg/mL of ZA with 1 mg/mL of the Erbitux); (4) this reaction generates an intermediate highly reactive that dissociates into free imidazole and a phosphoramidate composed of ZA conjugated with Erbitux at RT. Cet-ZA has been purified from the other free components of the reaction mixture (imidazole, EDC and ZA) through dialysis with the Slide-A-Lyzer Cassette (Thermo Fisher) at 10,000 molecular weight cut-off (MWCO) for 24 hours. The link between ZA and Cet is covalent in the absence of a linker molecule. Rituximab (Mabthera), was obtained as leftover as above and used to generate a Rit-ZA ADC with the same reaction sequence and chemical characterization used for Cet-ZA ADC.

Matrix assisted laser desorption ionization mass spectrometry and induction coupled plasma mass spectrometry

Matrix assisted laser desorption ionization mass spectrometry (MALDI-MS) was performed by Fondazione Toscana Life Sciences (Siena, Italy). The drug to antibody ratio (DAR) was estimated by MALDI-MS. The naked Cet (Erbitux) and the corresponding Cet-ZA ADC were desalted by SpinTrap G25 (Cytiva, Vancouver, Canada). 2 µL of desalted Cet or Cet-ZA ADC were mixed with 2 µL of a saturated solution of 2,5-dihydroxybenzoic acids-(DHB) in 0.1% trifluoroacetic acid (TFA) in acetonitrile:water (50:50, v/v). The resulting mixture was spotted on the MALDI target and left to dry in the air. Then 1 µL of the saturated matrix solution was added to each spot and left to dry. The mass spectra were acquired, over the mass range m/z 30–220 kDa, using a UltrafleXtreme (Bruker Daltonics, GmbH) in linear mode. A protein standard II calibration mixture (Bruker Daltonics, GmBH) was used for calibration. Induction coupled plasma (ICP)-MS was performed by Nanovex on samples treated with 2% HNO_3, using the 8900 ICP-QQQ Analyzer (Agilent Technologies, California, USA) to determine the amount of phosphorus (P) coupled to the antibody compared with the amount of sulfur (S).

Patients' specimens and organoids

Sixty-six patients suffering from CRC were studied (institutional informed consent signed at the time of surgery). The different tumor areas were determined by the staff of the Oncological Surgery Unit of the IRCCS Ospedale Policlinico San Martino. Tumor stage was determined according to the Union for International Cancer Control (UICC) and Dukes classification modified by Aster and Coller and microsatellite status was analyzed by the Pathology Unit.[27 28] Thirteen tumor specimens were also used for the generation of organoids and for the isolation of lymphocyte cell suspensions.

Primary CRC organoid cultures were obtained, as described, following published guidelines.[29 30] Tissue samples, were digested by collagenases type I and II in Leibovitz L15 medium (Gibco-Thermo Scientific), without serum and passed through a 100 µm strainer to eliminate residual matrix and mucus. Crypts were washed in fresh L15 medium to eliminate cell debris, mixed with Geltrex (lactose dehydrogenase elevating virus (LDEV)-free, human embryonic stem cells (hESC)-qualified, reduced growth factor; Gibco-Thermo), and plated in a 24-well plate. After polymerization at 37°C, Geltrex domes were covered with 500 µL of medium per well (Dulbecco's Modified Eagle Medium (DMEM-F12 with B27, epidermal grwoth factor (EGF) 25 ng/mL and A83-01 0.5 µM) supplemented with antibiotics. This method naturally selects pure colorectal epithelial cells within few in vitro passages, not allowing the expansion of other contaminating populations.[31 32] The absence of Wnt3a and R-spondin in the culture medium excluded the contamination of normal epithelial cells. Organoids used in this study are detailed in online supplemental table I. All these organoids have been used within the 8–9th culture passage. Some of them, such as the OMCR16-005TK and the OMCR18-025TK have been taken in culture until the 19th culture passage. The phenotypic features of all these organoids did not change along the culture period and they could be maintained in culture up to 6 months, without detectable signs of senescence or terminal differentiation. Some samples of digested tissue underwent density gradient centrifugation (Pancoll Human, 1.077 g/mL, PAN Biotech, Munich, Germany) resulting in >30% $CD45^+$ cells and about 60% epithelial cell adhesion molecule $(EPCAM)^+EGFR^+$ cells (not shown).

Western blot

Total proteins were extracted from CRC organoids (n=13) by radioimmunoprecipitation assay (RIPA) buffer; 8 µg protein/lane were resolved on Express Plus 4–16% gradient gels (GenScript, New Jersey, USA) and blotted on polyvinylidene fluoride (PVDF) membranes (GE-Healthcare, Milan, Italy). Antibodies: rabbit anti-BTN3A1 (Novus, Bio techne, Milan, Italy, NBP1-90750; 1:500 in tris buffered saline tween (TBST) 5% bovine serum albumin, BSA), rabbit anti-BTN2A1 (Bioss, Massachusetts, USA, bs-20473R; 1:1000 in TBST 5% skim milk), goat anti rabbit secondary antibody, horse radish peroxidase (HRP)-conjugated (Cell Signaling Technology, Massachusetts, USA, cat 7074; 1:2000 in TBST 5% BSA) and anti-beta-actin HRP-conjugated (Cell Signaling Technology, cat 5125; 1:10,000 in TBST 5% BSA) used as loading control. Protein bands were detected by chemiluminescent HRP substrate (Immobilon Western, Millipore, Massachusetts, USA) and acquired by Hyperfilm ECL (GE-Healthcare). Lanes density was quantified using the Image Studio Lite analysis software (LI-COR Biosciences, Nebraska, USA). BTN3A1 and BTN2A1 relative levels were normalized against beta-actin and plotted by Microsoft Excel software (Microsoft Corporation, Washington DC, USA).

IPP extraction and measurement

CRC organoids were seeded in 6-well plates (65 drops/well) and exposed to either 5 µM ZA or 2 µg/mL Cet-ZA for 48 hours. Cells were washed twice with cold phosphate-buffered saline (PBS), exposed to 500 µL ice-cold acetonitrile-LC grade Milli-Q water (3:2 v/v) and processed as described.[33] Cell extracts were evaporated in a SpeedVac (Savant, Thermo Fisher Scientific) and stored at −20°C until analysis. Then, extracts were dissolved in 80 µL Milli-Q water, 250 µL Na_3VO_4, cleared by centrifugation in MiniSpin Minifuge (Eppendorf, Germany; 13,000 rpm, 3 min) and transferred to liquid chromatography vials. Calibration curves for IPP were generated with standards diluted in Milli-Q water/0.25 mM Na_3VO_4 in the range 0.1–15 µM. IPP content was determined by high pressure liquid chromatography negative ion electrospray ionization time of flight mass spectrometry, operating in reflection negative ion mode, using an Agilent 1200

series chromatographic system.[34] For IPP determination, 5 µL of samples were injected onto a ZORBAX SB C18 column (150×0.5 mm, 5 µm particle size) (Agilent Technologies). The amount of IPP/dimethylallyl pyrophosphate, expressed as pmol/mg protein, was evaluated by calculating the peak area of the extracted ion current (m/z 244.99(M-H)$^-$), referred to a standard curve of IPP (range 0.1–15 µM) in control cell extracts. Total protein content was determined with the DC Protein Assay (Bio-Rad, California USA).

Flow cytometry and confocal microscopy

The CRC cell lines LS180, SW480, HT29, HCT116 and SW620 (provided and certified by Cell Bank Interlab Cell line Collection, IRCCS Policlinico San Martino) were incubated with serial dilutions (200–0.002 µg/mL/10^6 cells) of Cet or Cet-ZA ADC for 1 hour at RT, followed by the allophycocyanin (APC)-labeled anti-human Ig (APC-α-hIg) antiserum. Control aliquots were stained with APC-α-hIg. Organoids were disaggregated using trypsin-EDTA (Euroclone, Milan, Italy), washed with PBS and stained with either Cet or Cet-ZA ADC at 2 µg/mL/10^6 cells, followed by APC-α-hIg antiserum as above. Samples were analyzed by CyAn ADP flow cytometer (Beckman Coulter, Brea, California, USA) and results are expressed as log of mean fluorescence intensity (arbitrary units, a.u.) or percentage of positive cells. For confocal microscopy, LS180, SW480, HT29 or HCT116 cell lines were incubated with 2 µM Cet-ZA ADC for 1 hour at RT, followed by the APC-α-hIg antiserum and 100 nM SYTO 16 (Thermo Fisher Scientific), after seeding onto 96-well clear flat-bottomed black wall plates for imaging (Eppendorf). To detect the Cet-ZA internalization, samples of HCT116 cell line were incubated at 37°C for 1-5-24 hours, fixed with 1% paraformaldehyde (PFA), permeabilized with 1% Triton X-100, followed by APC-α-hIg antiserum, anti-lysosomal-associated membrane protein 1 (LAMP-1) mAb (clone H4A3, Thermo Fisher Scientific), followed by goat anti-mouse (GAM) anti-isotype specific Alexa Fluor 535 antiserum and SYTO 16 as above. Samples were observed with the PlanApo 40X NA1.40 oil objective with the FV500 confocal Laser Scanning Microscope System (Olympus Europe GmbH, Hamburg, Germany) equipped with an Argon, He-Ne green and He-Ne red lasers associated to IX81 motorized microscope (Olympus). Each image has been taken in sequence mode to avoid cross-contribution of each fluorochrome and data analyzed with FluoView V.4.3b computer software (Olympus). Results are shown in pseudocolor as red or green fluorescence versus nuclei in blue.

Vδ2 T-cell proliferation

Peripheral blood mononuclear cells (PBMC) were isolated from healthy donors (n=8) and patients with CRC (n=6) (institutional informed consent signed at the time of blood donation or at surgery) by density gradient centrifugation (Pancoll human), as described.[15] T lymphocytes were purified from PBMC using the specific negative separation kit (RosetteSep, STEMCELL Technologies, Vancouver, Canada) leading to >98% pure CD2$^+$CD3$^+$ T-cell populations and incubated overnight in Roswell Park Memorial Institute (RPMI) 1640 (supplemented with 10% fetal bovine serum, FBS, penicillin/streptomycin and L-glutamin, all from Gibco) to allow adherence of the residual undetectable monocyte component and avoid their presence in stimulation experiments. T lymphocytes were added to CRC organoids, previously seeded in 96-well/U-bottom plates (Sarstedt, Nümbrecht, Germany), in RPMI1640 complete medium as above. The ratio between T lymphocytes and organoid CRC cells, counted by flow cytometry (Miltenyi MACSQuant Cytofluorimeter, Bergisch Gladbach, Germany) in disaggregated parallel culture wells, was 10:1 (10^5T cells: 10^4 CRC cells in organoid) with 2 µg/mL Cet-ZA or 5 µM ZA. After 24 hours, human recombinant interleukin 2 (IL-2, PeproTech-Thermo Fisher Scientific, 30 IU/10 ng/mL final concentration) was added and co-cultures were continued at 37°C in a humidified 5% CO_2 incubator for up to 21 days. In some samples, 2 µg/mL Rit-ZA ADC was used as an additional control. Every 3 days, culture medium was replaced with fresh medium supplemented with IL-2. In some experiments, serial dilution of Cet-ZA (10–0.6 µg/mL/10^6 cells) was used to determine the EC_{50}. The amount of ZA, solubilized in dimethyl sulfoxid (DMSO) according to the manufacturer's recommendations, effective in Vδ2 stimulation was 0.5–5 µM[16 33]; at these concentrations, DMSO dilution was <1:10^3 and did not induce toxic effect as demonstrated by crystal-violet/propidium iodide assay.[35] The percentage of Vδ2 T cells was evaluated at 7, 14, 21 days of culture by double immunofluorescence with the anti-T-cell receptor (TCR) Vδ2 γδ123R3 (IgG1) and the anti-CD3 JT3A 289/11/F10 (IgG2a) mAb, followed by PE-GAM IgG1 or APC-GAM IgG2a (Thermo Fisher) and flow cytometry analysis (CyAN ADP Beckman Coulter or CytoFLEX Beckman Coulter).[15 16 35] Images of either CRC organoids, or T cells or co-cultures of organoid and T cells were taken using the JuLI-stage imaging recorder (NanoEnTeck, Gurogu, Seoul, South Korea). Cet-ZA ADC (2 µg/mL/10^6) was also used to stimulate CRC-derived cell suspensions: IL-2 was added after 24 hours and medium replaced every 3 days, as above. The percentage of Vδ2 T cells was evaluated at time 0 and at 7, 14, 21 days of culture by double immunofluorescence with the anti-Vδ2 γδ123R3 (IgG1) and the anti-CD45 (clone 9.4, IgG2a, American Type Culture Collection) mAb, followed by PE-GAM IgG1 or APC-GAM IgG2a (Thermo Fisher) and flow cytometry analysis.

Cytotoxicity and degranulation assays

Cytolytic activity exerted by Vδ2 T cells, in the presence of Cet-ZA, against CRC organoids, was performed with the crystal-violet assay as described.[16 35] Vδ2 T cells were isolated from patients or healthy donors' peripheral blood as described, and were 95% Vδ2$^+$ and 65%–95% CD16$^+$ (not shown).[16] Briefly, organoids were recovered from Geltrex drops (3 µL domes), put in 96-well/flat bottom

microplates (Greiner, Germany) and allowed to adhere for 24 hours in complete RPMI1640 medium. After this incubation the medium was changed and the organoids were co-cultured with autologous or allogenic Vδ2 T lymphocytes at different effector:target (E:T) ratios. Tumor cell number in representative wells was counted with the Miltenyi MACSQuant Cytofluorimeter, in order to calculate the E:T ratio. Experiments were then carried out without or with 2 µg/mL Cet-ZA, or 2 µg/mL Cet or 5 µM ZA; in some samples, the anti-Vδ2 mAb (γδ123R3) and/or the anti-CD16 (VD4) mAb were added, alone or in combination as indicated (each at the concentration of 1 µg/mL/10^6 effector cells). The expression of CD16 at the cell surface of Vδ2 T cells was assessed by flow cytometry (not shown) and only population with more than 60% of $CD16^+$ cells were used in these experiments. Incubation time was 48 hours to enable the entry of Vδ2 T lymphocytes into the organoids and the cytotoxicity.[16] To detect cytotoxicity, wells were stained with crystal-violet and colorimetric intensity evaluated at the wavelength of 594 nm with the fluorimeter VICTOR X5 (PerkinElmer Italia, Milan, Italy). These optical density (OD) values were compared with the OD values of the organoids cultured alone and referred to as 100% of viability.

In a second cytotoxicity assay, organoids were harvested by gently pipetting to limit their fragmentation but allowing disaggregation of the Geltrex dome. Then, 5×10^4 cells/well were seeded into 96-well black imaging plate clear-bottomed (Corning Incorporated-Sigma, Costar 3603) and allowed to adhere for 24 hours in an organoid medium. After adhesion, checked by microscopy, the organoid medium was replaced with RPMI1640 complete medium. Then, the fluorescent probe C. LIVE Tox Green reagent (25 nM, Cytena, Gothenburg, Sweden), was added and allowed to equilibrate for 24 hours. Finally, 10^5 Vδ2 T cells were added to the cultures, either with or without stimuli (ZA, Cet, Cet-ZA), and images taken in green pseudocolor every 6 hours for a period of 72 hours in bright field and green fluorescence channel, by the JuLI-Stage imaging recorder, to detect the increment of green fluorescence associated with cell killing. Images were converted into 8-bit grayscale pictures and analyzed with the Cell Counter plugin of the ImageJ2 computer program to measure fluorescence intensity evaluating the degree of gray nuances in a number or randomly distributed region of interest (ROI). In some experiments, anti-Vδ2 and/or anti-CD16 mAb (1 µg/mL) were added to block the engagement of the corresponding surface molecules and quantify the relative contribution of each receptor to the cytotoxic effect elicited by Vδ2 T cells.

Cytotoxic granule exocytosis by Vδ2 T cells towards organoids was tested by adding the APC-conjugated anti-CD107a mAb (LAMP-1, The Merck KGaA, Darmstadt, Germany) to the co-cultures performed as above (E:T ratio 2:1), either without or with 2 µg/mL Cet-ZA, for the last 24 hours. Cytolytic effectors were identified by staining with the FITC-anti-Vδ2 mAb (Miltenyi, Biotec, Germany). Samples underwent flow cytometry analysis (Cytoflex Beckman Coulter) and results expressed as percentage of $V\delta2^+CD107a^+$ cells.

Immunohistochemistry

Organoids were centrifuged at 200 rpm 1 min at RT, fixed overnight in HistoChoice MB (Sigma-Aldrich) containing 20% ethyl alcohol (ETOH), at 4°C, washed with PBS and suspended in 50 µL of melted agarose (2% in distilled water) in Eppendorf 1.5 mL tubes, to obtain small cones of agar filled with organoids that were processed for paraffin inclusion. Organoid samples or CRC biopsies (the latter fixed in 10% formalin overnight at 4°C) were dehydrated in a progressive series of ethanol, clarified in xylene and paraffin embedded. Four µm thick sections from CRC or organoids samples were cut and stained with the anti-Vδ2 mAb (1:100 BB3),[16] rabbit anti-BTN2A1 (1:300, Bioss Antibodies), rabbit anti-BTN3A1 (1:200, NovusBio), rabbit anti-villin 1 (VIL1) (1:400, Sigma-Aldrich), mouse anti-mucin 2 (MUC2) (1:400, Cell Marque-Sigma-Aldrich) or the mouse anti-chromogranin-A (CHGA) (1:1000, Sigma-Aldrich). Immunohistochemistry (IHC) was carried out using the automated stainer BOND RX (Leica Biosystem Italia, Milan, Italy), according to the manufacturer's instruction as follows: (1) de-paraffinization at 72°C for 30 min; (2) antigen retrieval with ER1 solution at 95°C for 10 min; (3) primary antibody staining, 20 min at 37°C; (4) Post Primary reagent (Leica) 8 min; (5) Polymer (Leica) 8 min; (6) Mixed DAB Refine (Leica) 8 min; (7) counterstaining with hematoxylin and mounting with Mount Quick Aqueous (Bio-Optica, Milan, Italy). Digital images were captured using the Aperio AT2 scanner (Leica) under 20× or 40× objective magnification and analyzed using the Aperio Scan Scope software (Leica Biosystems, Aperio Technologies).

Digital image analysis

In CRC sample analysis, the representative regions of interest were identified in the adenomatous tissue next to the luminal area of the tumor (LM-AD), in tumor luminal area (LM), central tumor (CT) and invasive tumor margin (IM) of each sample when available. BTN2A1 and BTN3A1 quantification were performed using the Cytoplasmic V2 macro of ImageScope software (Leica). The macro was developed with three intensity values of cut-off. The percentage of positive cells and the intensity of staining were reported as H-score (=3×%high+2×%middle+1× %low intensity stained cells; 0–300 range). $BB3^+$ cells were counted using the nuclear V9 algorithm of the ImageScope software tool (Leica). The nuclear algorithm was optimized for the identification of positive and negative cells. Results were reported as positive cells/total cells count/×100 or as the number of cells/mm^2. For organoids analysis, Aperio Cytoplasmic V2 and Membrane V9 macro were combined with a Genie pattern recognition macro to exclude background (mostly represented by residual agar Geltrex) from analysis. Genie software tool was trained to recognize organoids, glass or background. BTN3A1, BTN2A1, CHGA and

MUC2 expression were reported as H-score; VIL1 positive cells were counted using Membrane V9 macro. The algorithm was optimized for count positive 2+, 3+ and negative cells. Results were reported as the percentage of 2+ and 3+ cells/total cells/×100.

Statistical analysis

Data are presented as mean±SD as indicated. Statistical analysis was performed using one-tailed unpaired Student's t-test using the GraphPad Prism software V.5.0. The cut-off value of significance is indicated in each figure legend.

RESULTS

Characterization of Cet-ZA ADC

ZA conjugation with Cet was achieved following the scheme described for the chemical reactions occurring for nucleic acids and proteins, exploiting the synthesis of phosporamidate.[23–26] The reactions, leading to a covalent chemical bond between Cet and ZA, are summarized in online supplemental figure 1. Mass spectra of unconjugated native Cet and Cet-ZA ADC are depicted in figure 1A. MALDI mass spectra of both samples (Cet and Cet-ZA ADC) were characterized by multicharged species, in particular, the singly, doubly and triply charged species at about *m/z* 150 kDa, 75 kDa and 50 kDa, respectively. Successful covalent conjugation was confirmed by a positive mass shift of drug-loaded antibody in comparison to unconjugated one. In fact, the monocharged species for native Cet was detected at 152.2 kDa while for Cet-ZA ADC it was observed at 153.3 kDa (figure 1A, upper vs lower panel), with an increase in the MW of about 1100 units. The DAR was calculated from the difference in the measured masses for conjugate and unconjugated Cet divided for the expected mass change on the conjugation of one mole of ZA. The average measured DAR was 4.3, that is, 4.3 ZA molecules/1 Cet molecule. The amount of P, identifying ZA, compared with the amount of S, representative of Cet, determined by ICP-MS in the same samples used for MALDI analysis, is reported in online supplemental table II. The amount of P is very low in purified Cet and increases in Cet-ZA ADC by 886-fold; on the other hand, the amount of S is superimposable in Cet and Cet-ZA ADC preparations. MALDI and ICP-MS analyses indicate the successful covalent conjugation of ZA to Cet resulting in a Cet-ZA ADC.

To check the reactivity of Cet-ZA ADC, the $EGFR^{+}$ CRC cell lines LS180, SW480 and HT29 were incubated with serial dilution of the ADC, followed by APC-labeled anti-human Ig antiserum, and run on a flow cytometer. As shown in figure 1B, reactivity of the ADC on the three cell lines was similar to that of native Cet, optimal at 2 µg/mL/10^6 cells, concentration chosen for all functional experiments. Cet-ZA ADC barely reacted with the $EGFR^{dull}$ SW620 cell line (figure 1B lower panels). Membrane reactivity and cell distribution was also confirmed by confocal microscopy (figure 1C; red fluorescence: Cet-ZA ADC; blue pseudocolor: nuclei evidenced with SYTO 16 stain).

These data indicate that ZA conjugation does not alter Cet reactivity with EGFR and the Cet-ZA ADC maintains the same specificity of the native unconjugated antibody. Finally, both native Cet and Cet-ZA ADC internalization in HCT116 cell line (chosen for the high rate of EGFR recycling, not shown) started at 4 hours (not shown) and colocalization with the endosomal marker LAMP-1 was evident within 24 hours (online supplemental figure 2B vs 2A depicting the membrane reactivity of the Cet-ZA ADC).

Cet-ZA ADC reacts with CRC-derived organoids inducing IPP production

To confirm the reactivity of Cet-ZA ADC on primary CRC, organoids were obtained from 13 patients with CRC and cultured for functional assays. The characteristics of these organoids, and of the tumors of origin, are summarized in online supplemental table I: samples were anonymized with the acronym OMCR (Oncology Molecular, Colo-Rectal) followed by the year and progressive number of collection, and the letters T (tissue) and K (carcinoma). The organoids are referred to with the number only in all figures to avoid too long inscription (ie, OMCR18-025TK is reported as 18–025). All organoids display the morphology of epithelial cells organized in polarized three-dimensional (3D) structures and express epithelial cell markers such as VIL1, MUC2 and CHGA as depicted in online supplemental figure 3 (nine representative organoids shown) and all were positive for the human histocompatibility antigen human leukocyte antigen (HLA)-I and the EPCAM (not shown). Cet-ZA ADC could react by indirect immunofluorescence with these organoids, six of them depicted in figure 1D where reactivity is evaluated as cytofluorimetric analysis in fluorescence intensity and two reported in figure 1E as cell distribution in confocal microscopy.

Of note, exposure of CRC organoids with Cet-ZA ADC (2 µg/mL) for 48 hours, but not native Cet, resulted in the production of IPP documented by a significant increase ($p<0.02$) in IPP nM concentration in the three organoids tested (online supplemental table III), although lower than that elicited by soluble ZA. This indicates that ZA carried by the ADC can exert its metabolic effect. Moreover, all the organoids tested expressed BTN3A1 and BTN2A1 molecules, evaluated both by western blot (figure 2A, and densitometric analysis depicted in the lower panel) and by IHC (figure 2B, two representative cases). Figure 2C shows the expression of BTN3A1 and BTN2A1 in the tumor of origin of the two organoids depicted in B; this finding supports that in vitro cultured organoids can be considered representative of the tumor tissue. This was confirmed by digital pathology imaging whereby the expression of BTN3A1 and BTN2A1 molecules was measured in organoids and original tumors as described in online supplemental figure 4A,B. Indeed, the two BTNs were expressed by the organoids tested, although to a different extent, as documented by the H-score reported in the lower panels in figure 2. BTNs expression and IPP accumulation are necessary to get Vδ2 T lymphocytes activation and proliferation, making

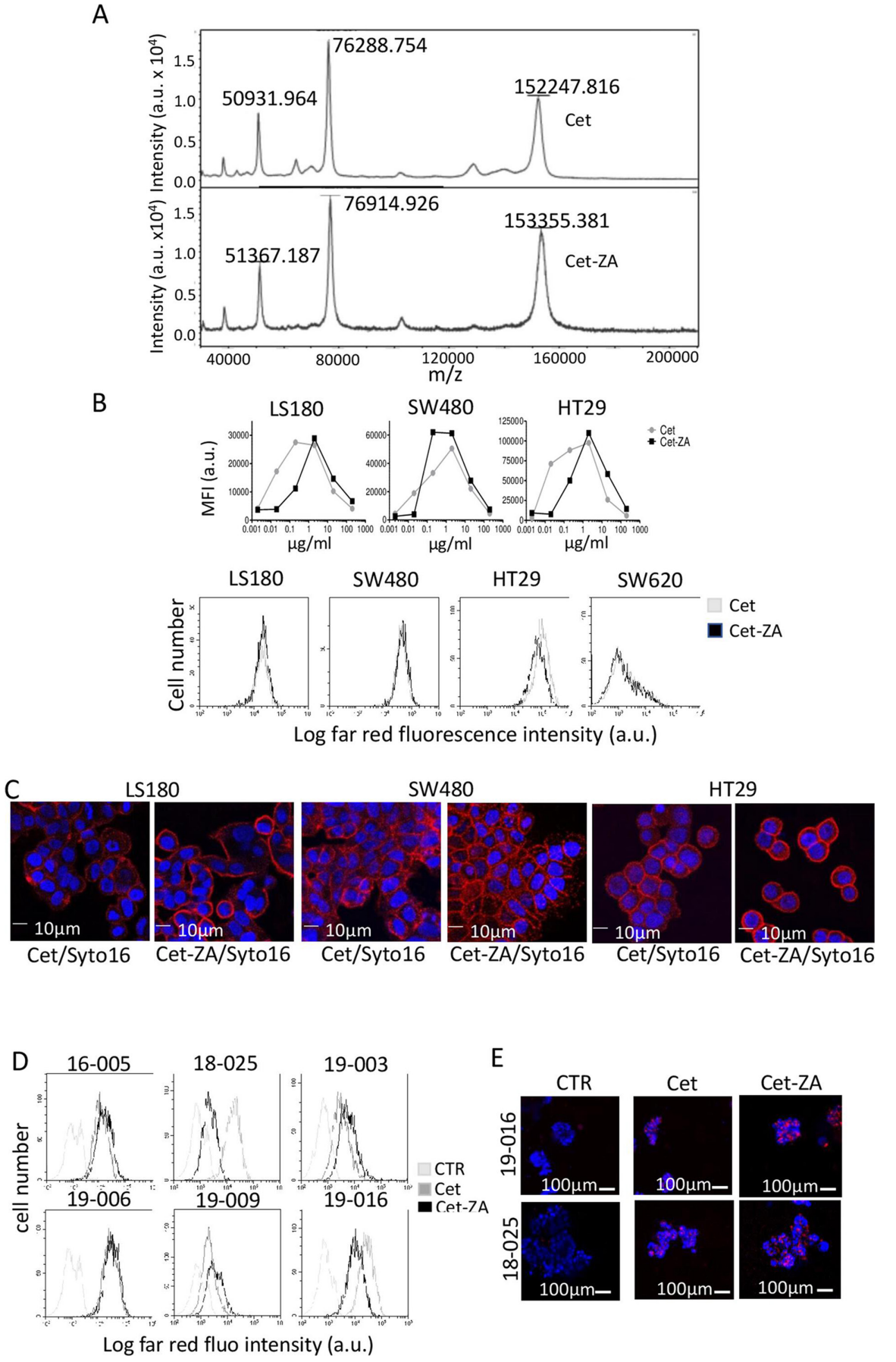

Figure 1 (Continued)

Figure 1 *Cet-ZA ADC characterization and reactivity with CRC organoids*. (A) Matrix assisted laser desorption ionization mass spectra of Cetuximab (top) and Cet-ZA ADC (bottom). Singly, doubly and triply charged species are detected at about m/z 150 kDa, 75 kDa and 50 kDa, respectively. (B) Cet-ZA titration. Upper panels: the CRC cell lines LS180, SW480 and HT29 were incubated with serial dilutions (200–0.002 µg/mL/10^6 cells) of Cet or Cet-ZA ADC for 1 hour at RT, followed by the APC-labeled anti-hIg antiserum. Samples were analyzed by CyAn ADP flow cytometer and results are expressed as log mean fluorescence intensity (MFI, arbitrary units, a.u.). Lower panels: histograms of the reactivity of Cet (light gray) or Cet-ZA ADC (black) at 2 µg/mL/10^6 cells evaluated by flow cytometry as above and expressed as log far red fluorescence intensity (a.u.) versus percentage of positive cells. Also, the epithelial growth factor receptor^{dull} SW620 cell line is depicted. Negative control (CTR; cells incubated with the APC-conjugated goat-human antiserum alone) is shown with the light gray line. (C) LS180, SW480, HT29 cell lines were incubated with 2 µg/mL Cet or Cet-ZA ADC as above followed by 100 nM SYTO 16, observed with FV500 Confocal Microscope (400× magnification) and data analyzed with FluoView V.4.3b computer software. Red: Cet or Cet-ZA. Blue: nuclei in pseudocolor. Bar: 10 µm. (D) The indicated organoids, prepared as described in Materials and Methods, were incubated with Cet (gray) or Cet-ZA ADC (black), followed by the APC-anti-hIg antiserum. Control aliquots were stained with APC-anti-hIg alone (CTR, light gray). Samples were analyzed by CyAn ADP flow cytometer and results are expressed as log far red fluorescence intensity (a.u.) versus cell number. (E) Organoids were incubated with 2 µg/mL Cet or Cet-ZA ADC as above followed by 100 nM SYTO 16, observed with FV500 Confocal Microscope (400× magnification) and data analyzed with FluoView V.4.3b computer software. Red: Cet or Cet-ZA. Blue: nuclei in pseudocolor. Bar:100 µm. ADC, antibody-drug conjugates; APC, allophycocyanin; Cet, cetuximab; CRC, colorectal cancer; RT, room temperature; ZA, zoledronic acid.

the organoid 3D system suitable for testing the functional effects of Cet-ZA ADC.

Cet-ZA ADC can stimulate Vδ2 T-cell growth and elicit antitumor cytotoxicity

In order to verify the hypothesis that Cet-ZA ADC can deliver ZA-mediated activation to Vδ2 T cells, T lymphocytes purified (>95% pure $CD2^+CD3^+$ T-cell populations) from PBMC (healthy donors: n=8, patients with CRC: n=6) were added to CRC organoids, at the ratio of 10:1 (10^5 T cells: 10^4 CRC cells in organoid), followed by the addition, after 24 hours, of 2 µg/mL Cet-ZA or 5 µM ZA and IL-2 (30 IU/10 ng/mL). Images of autologous cell cultures (16–005 organoid and T lymphocytes from the same patient), taken with the JuLI-stage imaging recorder (figure 3A), show increasing clumps of cells, at the different time points from day 7 to day 21, on treatment with 2 µg/mL Cet-ZA ADC.

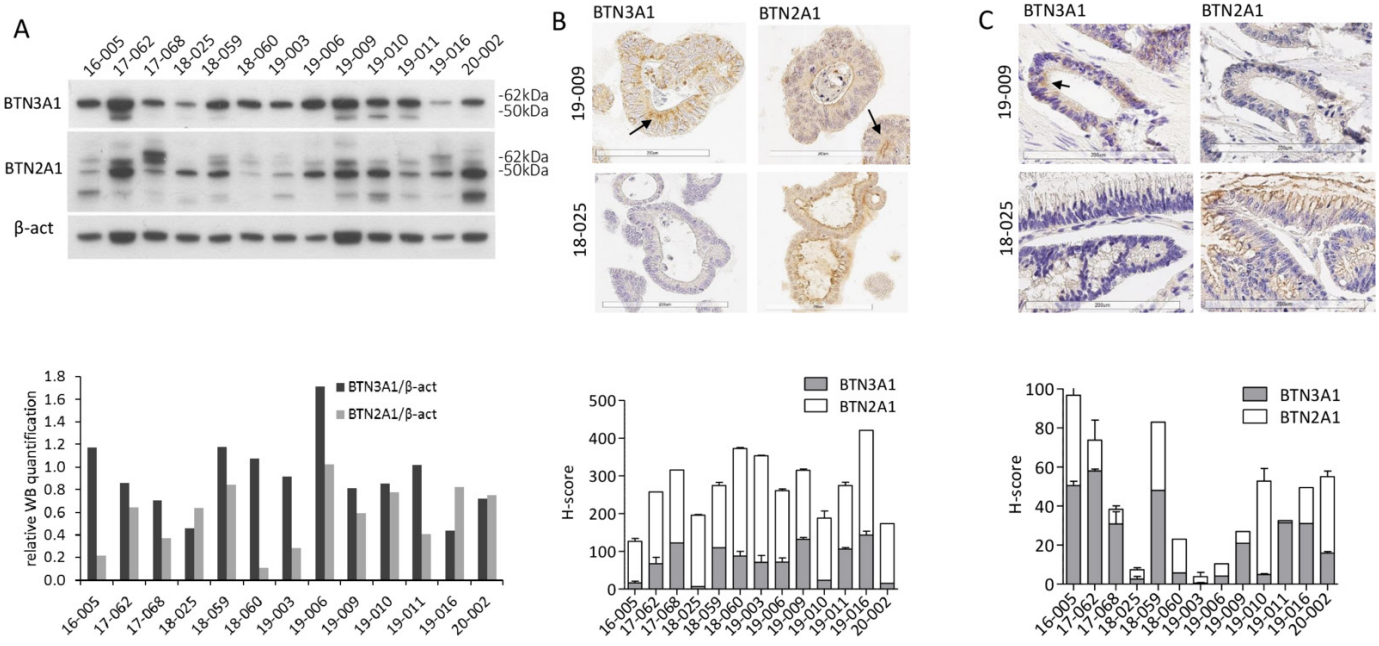

Figure 2 *Expression of BTN3A1 and BTN2A1 in CRC organoids*. (A) Upper panel: western blot of CRC organoid (n=13) lysates: BTN3A1, BTN2A1 and beta-actin signals are shown. Lower panel: histogram representing the relative quantification of BTN3A1 (black) and BTN2A1 (gray) levels, normalized against beta-actin. As BTN2A1 showed multiple bands, the lane with the higher signal (about 50 kDa) was used for quantification. (B) Upper pictures: expression of BTN3A1 and BTN2A1 by IHC on two representative CRC organoids (arrows indicate the main distribution). Lower panel: quantification (H-score) of BTN3A1 (gray) or BTN2A1 (white) expression in all CRC-derived organoids. Each value is the mean±SD from three different sections (each containing 20–40 organoids). (C) Upper pictures: expression of BTN3A1 and BTN2A1 by IHC on the tumor specimens where the organoids in (B) were derived from. Lower panel: quantification (H-score) of BTN3A1 (gray) or BTN2A1 (white) expression in all CRC specimens which organoids were derived from. Each value is the mean±SD from three different sections for each patient. BTN, butyrophilin; CRC, colorectal cancer; IHC, immunohistochemistry.

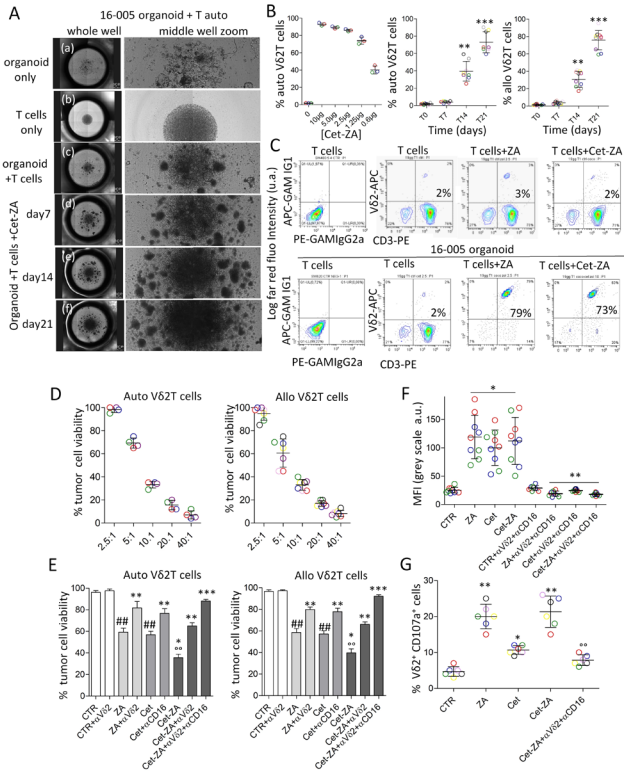

Figure 3 *Cet-ZA ADC can induce Vδ2 T-cell proliferation and trigger Vδ2 T-cell cytotoxicity against CRC organoids*. (A) Images of cell cultures of either CRC organoids, or autologous (auto) T cells or co-cultures of organoids and autologous T cells, taken using the JuLI-stage imaging recorder. For each culture condition, the combination of images of the entire well (left pictures) and the middle region of the U-bottomed culture well (right pictures) are shown. (A) organoids only at the onset of the assay; (B) T cells only on day 21 of culture; (C) T cells and organoids on day 21 of culture; (D–F) T cells and organoids in the presence of 2 µg/mL Cet-ZA on day 7, 14 and 21, respectively. (B) Percentage of Vδ2 T cells evaluated, by double immunofluorescence and FACS analysis at day 21 of culture with serial dilutions of Cet-ZA (0.6–10 µg/mL, left graph), or at day 7, 14, 21 of culture with 2 µg/mL Cet-ZA (central and right graphs). The different colors of the symbols represent organoids and T lymphocytes from different patients (central graph) or from different healthy donors (right graph). **p<0.001 and ***p<0.0001 versus T0 (day 0). (C) Percentage of Vδ2 T cells (upper panels: autologous T cells alone; lower panels: autologous T cells co-cultured with the 16–005 organoid), evaluated at day 21 of culture without or with 5 µM ZA, or 2 µg/mL Cet-ZA, by double immunofluorescence with the anti-Vδ2 γδ123R3 (IgG1) and the anti-CD3 JT3A 289/11/F10 (IgG2a) mAb, followed by PE-GAM IgG1 or APC-GAM IgG2a and fluorescence activated cell sorter (FACS) analysis. Negative controls of T cells incubated with both the anti-isotype specific GAM are shown in the left contour plots. Results are expressed as log far red fluorescence intensity (arbitrary units, a.u.) versus log red fluorescence intensity (a.u.). (D) Cytolytic activity exerted by autologous (left graph) or allogenic (right graph) Vδ2 T cells, at different effector:target (E:T) ratios, against CRC organoids seeded in Geltrex drops. After 72 hours, co-cultures were allowed to adhere in clean plates for further 24 hours, stained with crystal-violet and colorimetric intensity evaluated at 594 nm. Results are expressed as percentage of cell viability. Mean±SD from experiments performed with four (left) or six (right) organoids (different colors). (E) Cytolytic activity exerted by autologous (left graph) or allogenic (right graph) Vδ2 T cells, in the absence (control, CTR) or presence of 2 µg/mL Cet-ZA, or 2 µg/mL cet or 2 µM ZA, at the E:T ratio of 2.5:1. In some experiments, the anti(α)-Vδ2 mAb (γδ123) or the anti(α)-CD16 (VD4) mAb (1 µg/mL) were added, alone or in combination as indicated. Cytotoxicity was evaluated and results expressed as in panel (A). Mean±SD from experiments performed with four (left) or six (right) organoids. ##p<0.001 versus CTR; °°p<0.001 versus ZA or Cet; *p<0.0001 versus CTR; **p<0.001 versus ZA or Cet or Cet-ZA; ***p<0:0001 versus ZA or Cet or Cet-ZA. (F) Cytotoxicity measured on addition to CRC organoids/Vδ2 T-cell cultures of 100 nM C. LIVE Tox Green fluorescent probe for 24 hours, either without (CTR) or with stimuli (ZA, Cet, Cet-ZA), and in some samples with the anti(α)-Vδ2 plus anti(α)-CD16 mAb (1 µg/mL). Images were taken with the JuLI-stage imaging device, turned into black and white pictures and analyzed with the Cell Count plugin tool of the ImageJ2 software, after defining a random 200 region of interest. Results are expressed as mean fluorescence intensity as gray color intensity (a.u.) and are the mean±SD from three experiments, in triplicate, with nine different organoids (identified by colors) and autologous Vδ2 T cells. *p<0.001 versus CTR; **p<0.001 versus ZA, Cet, or Cet-ZA. (G) Cytotoxic granule exocytosis by Vδ2 T cells towards autologous organoids. The PE-conjugated anti-CD107a (LAMP-1) mAb was added to the co-cultures performed as above (E:T ratio 2.5:1), either without (CTR) or with ZA, Cet or Cet-ZA, for the last 24 hours. Cytolytic effectors were identified by staining with the APC-anti-CD3 mAb. Results are expressed as percentage of $CD3^+CD107a^+$ cells by flow cytometry analysis and are the mean±SD from five experiments (identified by colors) with different organoids and autologous Vδ2 T cells. **p<0.0001 versus CTR; *p<0.001 versus CTR; °°p<0.001 versus Cet-ZA. ADC, antibody-drug conjugates; APC, allophycocyanin; Cet, cetuximab; CRC, colorectal cancer; GAM, goat anti-mouse; LAMP-1, lysosomal-associated membrane protein 1; mAb, monoclonal antibodies; ZA, zoledronic acid.

These clumps are more evident than in co-cultures of CRC organoids and autologous T cells without the ADC. The percentage of Vδ2 T lymphocytes was evaluated, by double immunofluorescence and FACS analysis, at day 21 of culture with serial dilutions of Cet-ZA (0.6–10 µg/mL, figure 3B left graph) and revealed the dose of 1 µg/mL as EC_{50} of Cet-ZA ADC (80% Vδ2 T cells on day 21 vs <5% of the initial T-cell composition at day 0). On day 14 and 21 of culture, a significant increase in the percentage of Vδ2 T cells could be found both in autologous cultures (figure 3B, central graph) and in cultures performed with CRC organoids and allogenic T lymphocytes (figure 3B, right graph) in the presence of 2 µg/mL Cet-ZA. The effect of Cet-ZA ADC on Vδ2 T-cell increase was superimposable to that obtained with soluble ZA at the concentration of 5 µM (figure 3C, lower right and lower central panels). No increase in Vδ2 T-cell number was observed using Rit-ZA ADC (not shown). Then, we analyzed whether Cet-ZA could trigger Vδ2 T cells to exert effective cytotoxic activity. CRC organoids were co-cultured with autologous or allogenic Vδ2 T lymphocytes (figure 3D, left and right graphs, respectively), at different E:T ratios, for 72 hours to enable the entry of Vδ2 T lymphocytes into the domes and initiate the cytotoxicity. Since at the ratio of 2.5:1 Vδ2 T cells did not exert spontaneous cytotoxicity (tumor cell viability in figure 3D), this ratio was chosen for further experiments with Cet-ZA ADC, or native Cet, to allow the detection of Cet-ZA/ADCC effect mediated via TCR or FcγRIIIA (CD16), respectively. Figure 3E shows that the percentage of viable tumor cells from CRC organoids significantly decreased up to 40% in co-cultures with autologous (left graph) or allogenic (right graph) Vδ2 T lymphocytes in the presence of Cet-ZA, and this effect was significantly stronger than that obtained with native Cet or soluble ZA (60% of viable CRC cells). It is of note that the combination of the anti-Vδ2 TCR mAb and the anti-CD16 mAb could neutralize Cet-ZA-induced cytotoxicity that in turn was inhibited by 20–30% when the anti-Vδ2 TCR mAb was used alone (figure 3E). This data indicates that Cet-ZA can activate tumor cell killing by both TCR and FcγRIIIA. On the other hand, the anti-Vδ2 TCR or the anti-CD16 mAb could inhibit either ZA or Cet-induced cytotoxicity, respectively (figure 3E).

Superimposable results were obtained by a different cytotoxicity assay based on the ability of the C. LIVE Tox Green fluorescent probe to mark dead cells. CRC organoids were co-cultured with Vδ2 T cells, either without (CTR) or with stimuli (ZA, Cet, Cet-ZA), and in some samples with the anti-Vδ2 and/or anti-CD16 mAb. To evaluate cytotoxicity, images were taken every 6 hours in bright field and with the green fluorescence channel of the JuLI-stage imaging recorder, with automatic focus and without threshold modifications or any other manipulations (online supplemental figure 5A showing both dark and bright fields). Images were then turned into black and white pictures and analyzed with the Cell Count plugin of the ImageJ2 computer program to measure fluorescence intensity evaluating the degree of gray nuances, after defining 200 ROI on the black and white images (online supplemental figure 5B). As shown in figure 3F, an increment of fluorescence, expressed as color intensity (a.u.), associated with cell killing was detected mainly in the presence of Cet-ZA ADC. Also, in this system, anti-Vδ2 and/or anti-CD16 mAb, added to block the engagement of the corresponding surface molecules, resulted in the inhibition of the cytotoxic effect exerted by autologous Vδ2 T cells (figure 3F; online supplemental figure 5A lower panels). To verify the activation of effector cells, we analyzed the degranulation of cytotoxic vesicles by evaluating the exposure of the LAMP-1/CD107a at the surface of Vδ2 T cells, that accompanies the release of lytic granule contents.[36] Cytotoxic granule exocytosis by Vδ2 cells towards autologous organoids (E:T ratio 2:1) was evidenced by flow cytometry and expressed as percentage of $CD3^+CD107a^+$ cells. As shown in figure 3G, $CD3^+CD107a^+$ cells significantly increased in the presence of 2 µg/mL Cet-ZA and this effect was strongly impaired by the combination of anti-Vδ2 and anti-CD16 mAbs. These findings confirmed that the ADC can activate and trigger the degranulation of cytolytic enzymes, on interaction with CRC organoids, through the engagement of TCR and FcγRIIIA (CD16).

Vδ2 T cells are localized in CRC areas expressing BTN3A1 or BTN2A1

To prove the potential recruitment of antitumor γδ effector T lymphocytes by Cet-ZA ADC in patients with CRC, the presence of Vδ2 T cells and BTNs at the tumor site were analyzed by IHC in 66 CRC samples. Both BTN3A1 or BTN2A1 expression and the localization of Vδ2 T lymphocytes were examined by digital pathology in selected tumor areas, defined as explained in online supplemental figure 6: LM-AD, LM, CT and IM. BTN3A1 is significantly expressed mainly in LM and CT zones (online supplemental figure 6B left graph and panel C), while BTN2A1 is represented in all tumor and adenomatous areas (online supplemental figure 6B, right graph). Interestingly, Vδ2 T lymphocytes can be found both in adenomatous and in tumor areas, mainly in LM and CT (figure 4A: 1 representative case and figure 4B: 66 cases). Vδ2 T lymphocytes were counted both as percentage of cells compared with the total nuclear count (figure 4B, left graph), as explained in online supplemental figure 4C, or as number of cells/mm^2 (figure 4B, right graph, as described in Materials and Methods). In both evaluations, Vδ2 T lymphocytes can be found not only close to the tumor (LM-AD), but also inside the tumor (LM and CT), where BTNs, in particular BTN3A1, are expressed (online supplemental figure 6B,C). To evaluate the stimulatory effect of Cet-ZA ADC on infiltrating γδ T lymphocytes, cell suspensions obtained from tumor specimens of 10 patients with CRC and used in functional experiments. Vδ2 T cells were identified by double immunofluorescence with the anti-TCR Vδ2 γδ123R3 and the anti-CD45 mAbs and flow cytometry analysis. Of note, CRC-derived cell suspensions cultured with Cet-ZA ADC

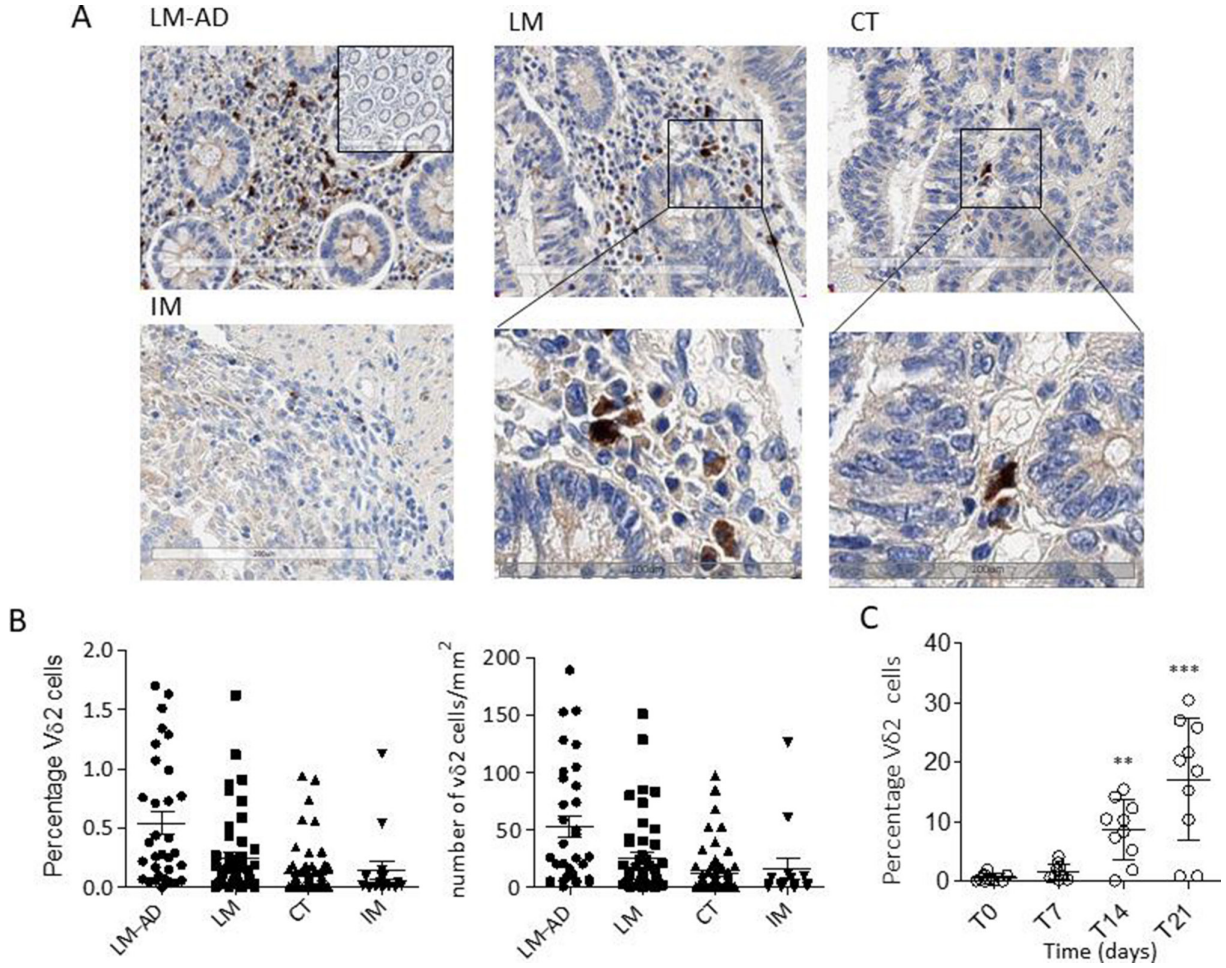

Figure 4 *CRC localization of Vδ2 T lymphocytes in different tumor areas*. (A) Vδ2 T lymphocyte identified by staining with the anti-Vδ2 BB3 mAb in the different areas of a representative CRC. Upper images: adenomatous areas (LM-AD, left), luminal margin (LM, central) or central tumor (CT, right) (20× magnification). Inset in the upper left image: negative CTR with the second reagents alone (10×). Lower left image: invasive margin (IM), lower central and lower right images are enlargements of the squares indicated in LM and CT of the upper images. (B) Quantification of Vδ2 T-cell infiltration in patients with CRC: LM-AD, LM, CT and IM, evaluated with the Nuclear V9 macro of Leica Image Scope V.12.3 software (described in online supplemental figure 4C). Left graph: percentage of Vδ2 T lymphocytes/total cell number (nuclei count). Right graph: number of Vδ2 T lymphocytes/mm^2. (C) Cet-ZA ADC (2 µg/mL/10^6 cells) was added to CRC-derived cell suspensions and Vδ2 T cells were evaluated at time 0 and at 7, 14, 21 days of culture by double immunofluorescence with the anti-Vδ2 mAb γδ123R3 and the anti-CD45 mAb, followed by PE-GAM IgG1 or APC-GAM IgG2a and flow cytometry analysis. Results are expressed as percentage of Vδ2 T cells as mean±SD from 10 cases. **p<0.001 and ***p<0.0001 versus T0 (day 0). ADC, antibody-drug conjugates; APC, allophycocyanin; Cet, cetuximab; CRC, colorectal cancer; GAM, goat anti-mouse; mAB, monoclonal antibodies; ZA, zoledronic acid.

resulted in a significant increase of Vδ2 T lymphocytes at 14 and 21 days of culture (figure 4C), indicating that the tumor infiltrating Vδ2 T-cell subset is sensitive to the stimulating action of the ADC.

DISCUSSION

We developed a new ADC made of a small molecule (ZA), able to trigger a subset of antitumor T lymphocytes (Vδ2 T cells), linked to a mAb (Cet) targeting EGFR on CRC. ADC are promising therapeutic compounds, that achieve the old scientific concept of 'magic bullets,' which was described by Paul Ehrlich over 100 years ago, to hit selectively a specific target.[37] However, less than 1% of the currently administered ADC is expected to target the tumor.[20 21] In most cases, ADC are composed of specific mAb linked to a toxin/antimitotic drug or to inhibitors of DNA-regulating enzymes.[38–40] Peculiar ADC are the immunocytokine-drug conjugates (IDC), which combine a tumor-homing antibody, a cytotoxic drug and a cytokine in the same molecular entity.[41] As an example, a trifunctional ADC carrying IL-12, capable of inducing activation and proliferation of T and natural killer lymphocytes, has been reported.[42]

In any case, none of these ADC or IDC is aimed to select an effector cell population and drive it directly to the tumor. We propose a novel approach that, in principle, allows the

activation of an antitumor immune response leading the selected effector cells to the target and achieving a precise localization of cancer cytotoxicity. Cet-ZA seems to meet these requirements; indeed, the antibody specificity enables the ADC to carry ZA into the tumor cells that become stimulators of effectors γδ T cells through the production of IPP elicited by the bisphosphonate.

ZA conjugation with Cet was obtained exploiting the chemical reactions occurring for nucleic acids and proteins, through the synthesis of phosphoramidate linking a small molecule to an antibody.[23 24] This covalent link makes Cet-ZA similar to second generation ADC, with the advantage of stability and free antibody binding site (compared with the first or the third-generation ADC, respectively[38]) that may favor tumor targeting. In general, ADC are designed for internalization and are processed as the antibodies via the endocytic pathway resulting in intracellular effect of the payload.[43] Accordingly, Cet-ZA is internalized in CRC cells, colocalized with the endocytic marker LAMP-1. A pH-cleavable phosphoramidate linker for the conjugation of monomethyl auristantin E in ADC has been reported to have high stability at physiological pH, releasing its payload at acidic pH.[44] Moreover, the reactivity of the ADC is preserved both on CRC cell lines and organoids. This would allow this ADC to reach the target that is represented not only by single cells, as may occur in metastatic process, but also by cell aggregates as in growing tumors.

From this viewpoint, primary organoids derived from epithelial tumors are emerging as reliable 3D culture system; despite they lack a full tissue architecture, several studies increasingly support the use of this 3D model for cancer biology and pharmacological studies.[29–32] Three-D systems for preclinical studies have evolved in the last years to reproduce microenvironment in the study of anticancer treatments.[45 46] Indeed, tumor development in humans is not always fully reproducible and predictable in animal models; also, they are very expensive and often show a negative environmental impact.[47–49] Thus, several 3D culture systems, have been validated by the European Union Reference Laboratories for Alternatives to Animal Testing (EURL ECVAM) as preclinical models, as they offer many advantages such as reproducibility, low costs, high number of replicates, simultaneous evaluation of multiple parameters and standardized co-cultures with different cell types.[50–52]

In particular in our model, besides epithelial and CRC markers, BTN3A molecules are expressed on organoids, that are able to produce IPP, making this system feasible and reliable to detect ZA effects. Indeed, Cet-ZA ADC is efficient in inducing γδ T-cell proliferation in co-cultures of autologous or allogenic T lymphocytes and CRC organoids, provided their expression of BTN3A1/2 molecules, through IPP production and Vδ2 TCR engagement.[6 7 13] It is noteworthy that Cet-ZA triggers the proliferation of autologous Vδ2 T cells, including those derived by the tumor; moreover, the ADC can induce Vδ2 T lymphocytes to exert cytotoxicity (at an E:T ratio where spontaneous killing is not active) against tumor organoids, that represent reliable fragments of the original tumor. Interestingly, Cet-ZA ADC can elicit both TCR-mediated cytotoxicity, due to ZA effect, and ADCC due to Cet binding to FcγRIIIA/CD16 thus providing a double weapon to kill tumor cells. The finding that also allogenic T cells can be activated by Cet-ZA ADC is remarkable as allo-γδ T lymphocytes have been used in some immunotherapeutic schemes, due to their low spontaneous alloreactivity (against healthy tissues), although the clinical outcome is not always satisfactory.[52] Nevertheless, allo-T lymphocytes offer the opportunity to prepare and store antitumor effector cells in advance of the time when it would be difficult to generate them from a patient with cancer.

Also, we can speculate that the triggering of Vδ2 T cells against CRC can be enhanced by blocking the function of immune checkpoint receptors such as programmed cell death protein-1 (PD-1). In fact, we found that the infiltrating Vδ2 T cells expressing PD-1 were usually less than 15% (range 2.2–14.6% n=10) as well as the percentage of PD-1^{+} activated Vδ2 T cells obtained from co-cultures with organoids (not shown). This would suggest that PD-1 can play a minor role in regulating Vδ2 T cells. Nevertheless, several other inhibitory receptors can be expressed on antitumor effector lymphocytes[53] and further studies on this topic are needed to define their functional role on Vδ2 T cells.

In most patients analyzed in this study, γδ T cells and BTN3A1 are present and expressed in the center of CRC, making it possible to elicit their function on administration of the ADC. Indeed, expression of BTNs, mainly BTN3A1, are essential for the recognition of phosphoantigens by γδ T lymphocytes, due to the B30.2 binding domain.[12–15] In particular, IHC showed that BTN3A1 can be detected on tumor cells close to areas infiltrated by Vδ2 T lymphocytes, in the same patients from which the organoids were derived. These data support that Cet-ZA could work as antitumor ADC in vivo and immunohistochemical analysis of BTN3A1 expression at the tumor site can help to select patients with CRC potentially responders to such treatment.

CONCLUSIONS

Despite the incompletely achieved clinical results, ADC remain promising therapeutic tools in cancer therapy. The Cet-ZA ADC, herein described, can represent an additional tool in the field, showing immunostimulant properties and maintaining the original specificity of the antibody. The most powerful characteristic of this ADC is the ability to select an effector T-cell population activating both TCR-elicited tumor cell killing and conventional ADCC. This should result in a precise and effective targeting of CRC, favoring the development of a double-edged antitumor immune response that, in principle, would amplify the therapeutic effect. In addition, organoids from patients with CRC, together with autologous T lymphocytes, conceivably provide a feasible, low cost, reliable and reproducible 3D model, to use as a tailored preclinical therapeutic assay.

Acknowledgements We thank Damiana La Torre and Claudio Malfatto for technical assistance, Aldo Profumo MSc (Proteomic Unit IRCCS Ospedale Policlinico San Martino), Elisa Nuti PhD and Armando Rossello PhD (Department of Pharmacology, University of Pisa) for helpful discussion and support.

Contributors RB derived colorectal carcinoma organoids, performed immunohistochemistry (IHC) experiments and image analysis, WB assays, and wrote the corresponding sections revised. DC performed isopentenyl pyrophosphates (IPP) production experiments and IHC experiments and image analysis. LS performed the mass spectrometry analyses and wrote the relative section. ST performed the confocal experiments and organized the figures relative to confocal microscopy. FT performed the IPP production experiments and wrote the relative section. FV performed generation of Vδ2 T cells and co-culture experiments. MRZ wrote the first draft of the manuscript and planned all the experiments shown. AP performed generation of Vδ2 T cells, the co-culture experiments for Vδ2 expansion, ideation of the generation of the new antibody-drug conjugate, planned and analyzed the cytotoxic experiments, some confocal microscopy experiments, planned the experiments with MRZ organized and granted the manuscript. All the authors revised the manuscript. AP accepts the full responsibility for this work and he acts as guarantor.

Funding This study has been supported by the AIRC IG-21648, Compagnia di San Paolo (ROL 32567), 5xmille 2015 and 2016 and Ricerca Corrente from the Italian Ministry of Health to AP.

Competing interests None declared.

Patient consent for publication Not applicable.

Ethics approval This study involves human participants and was approved by PR163REG201, renewed in 2017, Ethics Committee Approval For Liguria Region. Participants gave informed consent to participate in the study before taking part.

Provenance and peer review Not commissioned; externally peer reviewed.

Data availability statement Data are available upon reasonable request. All data relevant to the study are included in the article or uploaded as supplementary information.

ORCID iD

Alessandro Poggi http://orcid.org/0000-0002-1860-430X

REFERENCES

1 Fridman WH, Pagès F, Sautès-Fridman C, *et al*. The immune contexture in human tumours: impact on clinical outcome. *Nat Rev Cancer* 2012;12:298–306.
2 Church SE, Galon J. Tumor microenvironment and immunotherapy: the whole picture is better than a glimpse. *Immunity* 2015;43:631–3.
3 Gentles AJ, Newman AM, Liu CL, *et al*. The prognostic landscape of genes and infiltrating immune cells across human cancers. *Nat Med* 2015;21:938–45.
4 Meraviglia S, Lo Presti E, Tosolini M, *et al*. Distinctive features of tumor-infiltrating γδ T lymphocytes in human colorectal cancer. *Oncoimmunology* 2017;6:e1347742.
5 Corvaisier M, Moreau-Aubry A, Diez E, *et al*. V gamma 9V delta 2 T cell response to colon carcinoma cells. *J Immunol* 2005;175:5481–8.
6 Bonneville M, O'Brien RL, Born WK. Gammadelta T cell effector functions: a blend of innate programming and acquired plasticity. *Nat Rev Immunol* 2010;10:467–78.
7 Poggi A, Zocchi MR. γδT Lymphocytes as a first line of immune defense: old and new ways of antigen recognition and implications for cancer immunotherapy. *Front Immunol* 2014;5:575.
8 Bhat J, Kabelitz D. γδ T cells and epigenetic drugs: A useful merger in cancer immunotherapy? *Oncoimmunology* 2015;4:e1006088.
9 Kabelitz D, Wesch D, He W. Perspectives of gammadelta T cells in tumor immunology. *Cancer Res* 2007;67:5–8.
10 Santini D, Vespasiani Gentilucci U, Vincenzi B, *et al*. The antineoplastic role of bisphosphonates: from basic research to clinical evidence. *Ann Oncol* 2003;14:1468–76.
11 Santolaria T, Robard M, Léger A, *et al*. Repeated systemic administrations of both aminobisphosphonates and human Vγ9Vδ2 T cells efficiently control tumor development in vivo. *J Immunol* 2013;191:1993–2000.
12 Arnett HA, Viney JL. Immune modulation by butyrophilins. *Nat Rev Immunol* 2014;14:559–69.
13 Vavassori S, Kumar A, Wan GS, *et al*. Butyrophilin 3A1 binds phosphorylated antigens and stimulates human γδ T cells. *Nat Immunol* 2013;14:908–16.
14 Cano CE, Pasero C, De Gassart A, *et al*. BTN2A1, an immune checkpoint targeting Vγ9Vδ2 T cell cytotoxicity against malignant cells. *Cell Rep* 2021;36:109359.
15 Zocchi MR, Costa D, Venè R, *et al*. Zoledronate can induce colorectal cancer microenvironment expressing BTN3A1 to stimulate effector γδ T cells with antitumor activity. *Oncoimmunology* 2017;6:e1278099:3.
16 Di Mascolo D, Varesano S, Benelli R, *et al*. Nanoformulated zoledronic acid boosts the Vδ2 T cell immunotherapeutic potential in colorectal cancer. *Cancers* 2019;12:104.
17 Gong J, Cho M, Fakih M. Ras and BRAF in metastatic colorectal cancer management. *J Gastrointest Oncol* 2016;7:687–704.
18 Grothey A, Sargent DJ. Adjuvant therapy for colon cancer: small steps toward precision medicine. *JAMA Oncol* 2016;2:1133–4.
19 Chen Y, Liu G, Guo L, *et al*. Enhancement of tumor uptake and therapeutic efficacy of EGFR-targeted antibody cetuximab and antibody-drug conjugates by cholesterol sequestration. *Int J Cancer* 2015;136:182–94.
20 Agarwal P, Bertozzi CR. Site-specific antibody-drug conjugates: the nexus of bioorthogonal chemistry, protein engineering, and drug development. *Bioconjug Chem* 2015;26:176–92.
21 Sapra P, Stein R, Pickett J, *et al*. Anti-CD74 antibody-doxorubicin conjugate, IMMU-110, in a human multiple myeloma xenograft and in monkeys. *Clin Cancer Res* 2005;11:5257–64.
22 Tiberghien AC, Levy J-N, Masterson LA, *et al*. Design and synthesis of Tesirine, a clinical antibody-drug conjugate pyrrolobenzodiazepine dimer Payload. *ACS Med Chem Lett* 2016;7:983–7.
23 Ghosh SS, Kao PM, McCue AW, *et al*. Use of maleimide-thiol coupling chemistry for efficient syntheses of oligonucleotide-enzyme conjugate hybridization probes. *Bioconjug Chem* 1990;1:71–6.
24 Shabarova ZA, Ivanovskaya MG, Isaguliants MG. DNA-like duplexes with repetitions: efficient template-guided polycondensation of decadeoxyribonucleotide imidazolide. *FEBS Lett* 1983;154:288–92.
25 Shabarova ZA. Synthetic nucleotide-peptides. *Prog Nucleic Acid Res Mol Biol* 1970;10:145–82.
26 Itumoh EJ, Data S, Leitao EM. Opening up the toolbox: synthesis and mechanisms of phosphoramidates. *Molecules* 2020;25:3684.
27 Astler VB, Coller FA. The prognostic significance of direct extension of carcinoma of the colon and rectum. *Ann Surg* 1954;139:846–52.
28 Guinney J, Dienstmann R, Wang X, *et al*. The consensus molecular subtypes of colorectal cancer. *Nat Med* 2015;21:1350–6.
29 van de Wetering M, Francies HE, Francis JM, *et al*. Prospective derivation of a living organoid biobank of colorectal cancer patients. *Cell* 2015;161:933–45.
30 Fujii M, Shimokawa M, Date S, *et al*. A colorectal tumor organoid library demonstrates progressive loss of niche factor requirements during tumorigenesis. *Cell Stem Cell* 2016;18:827–38.
31 Neal JT, Li X, Zhu J, *et al*. Organoid modeling of the tumor immune microenvironment. *Cell* 2018;175:1972–88.
32 Sato T, Stange DE, Ferrante M, *et al*. Long-term expansion of epithelial organoids from human colon, adenoma, adenocarcinoma, and Barrett's epithelium. *Gastroenterology* 2011;141:1762–72.
33 Jauhiainen M, Mönkkönen H, Räikkönen J, *et al*. Analysis of endogenous ATP analogs and mevalonate pathway metabolites in cancer cell cultures using liquid chromatography–electrospray ionization mass spectrometry. *J Chromatogr B* 2009;877:2967–75.
34 Tosetti F, Venè R, Camodeca C, *et al*. Specific ADAM10 inhibitors localize in exosome-like vesicles released by Hodgkin lymphoma and stromal cells and prevent sheddase activity carried to bystander cells. *Oncoimmunology* 2018;7:e1421889.
35 Varesano S, Zocchi MR, Poggi A. Zoledronate triggers Vδ2 T cells to destroy and kill spheroids of colon carcinoma: quantitative image analysis of three-dimensional cultures. *Front Immunol* 2018;9:998.

36 Poggi A, Catellani S, Garuti A, *et al*. Effective in vivo induction of NKG2D ligands in acute myeloid leukaemias by all-trans-retinoic acid or sodium valproate. *Leukemia* 2009;23:641–8.
37 Erlich P. *Experimental researches on specific therapy: on immunity with special reference to the relationship between distribution and action of antigens" from ''The Harben Lectures for 1907 of the Royal Institute of Public Health''*. London: Lewis, 1908.
38 Beck A, Goetsch L, Dumontet C, *et al*. Strategies and challenges for the next generation of antibody-drug conjugates. *Nat Rev Drug Discov* 2017;16:315–37.
39 Baah S, Laws M, Rahman KM. Antibody-Drug Conjugates-A tutorial review. *Molecules* 2021;26:2943.
40 Cianferotti C, Faltoni V, Cini E, *et al*. Antibody drug conjugates with hydroxamic acid cargos for histone deacetylase (HDAC) inhibition. *Chem Commun* 2021;57:867–70.
41 Khattak ZE, Hashmi H, Khan SI, *et al*. Dawn of a new era of antibody-drug conjugates and bispecific T-cell engagers for treatment of multiple myeloma: a systematic review of literature. *Ann Hematol* 2021;100:2155–72.
42 List T, Casi G, Neri D. A chemically defined trifunctional antibody-cytokine-drug conjugate with potent antitumor activity. *Mol Cancer Ther* 2014;13:2641–52.
43 Dean AQ, Luo S, Twomey JD, *et al*. Targeting cancer with antibody-drug conjugates: promises and challenges. *MAbs* 2021;13:1951427.
44 Olatunji FP, Herman JW, Kesic BN, *et al*. A click-ready pH-triggered phosphoramidate-based linker for controlled release of monomethyl auristatin E. *Tetrahedron Lett* 2020;61:152398.
45 Hirata E, Sahai E. Tumor microenvironment and differential responses to therapy. *Cold Spring Harb Perspect Med* 2017;7:a026781.
46 Wu T, Dai Y. Tumor microenvironment and therapeutic response. *Cancer Lett* 2017;387:61–8.
47 Akhtar A. The flaws and human harms of animal experimentation. *Camb Q Healthc Ethics* 2015;24:407–19.
48 Enna SJ, Williams M. Defining the role of pharmacology in the emerging world of translational research. *Adv Pharmacol* 2009;57:1–30.
49 Ellis LM, Fidler IJ. Finding the tumor copycat. Therapy fails, patients don't. *Nat Med* 2010;16:974–5.
50 Verjans E-T, Doijen J, Luyten W, *et al*. Three-dimensional cell culture models for anticancer drug screening: worth the effort? *J Cell Physiol* 2018;233:2993–3003.
51 Cox MC, Reese LM, Bickford LR, *et al*. Toward the broad adoption of 3D tumor models in the cancer drug pipeline. *ACS Biomater Sci Eng* 2015;1:877–94.
52 Morrison AL, Campagna A, Bodman-Smith M. Sometimes simple is not best: the complex γδ T cell interaction with tumor need depth. *Clin. Transl. Disc* 2022;2:e71.
53 Poggi A, Zocchi MR. Natural killer cells and immune-checkpoint inhibitor therapy: current knowledge and new challenges. *Mol Ther Oncolytics* 2022;24:26–42.